J. GUTEK[1], S. WINIARZ[1], I. PIECHOCKA[1], P. PŁOTKA[2], R. CZAJKA[1]

[1] Poznań University of Technology
Faculty of Technical Physics, Institute of Physics
Poland, e-mail: czajka@phys.put.poznan.pl
[2]Institute for Semiconductor Research, Sendai, Japan

INVESTIGATIONS OF THE COULOMB BLOCKADE EFFECT IN DOUBLE TUNNEL JUNCTIONS

The Coulomb Blockade effect (CBE) is observed in double tunnel junctions where a small metallic cluster is precisely located between two outer electrodes. This electrically isolated nanocluster exhibits capacitances of attofarads. Such extremely small capacitance may cause that the charging energy $E_C = e^2/2C$ which an individual electron needs to be placed at the cluster may be bigger than the electron's thermal energy k_BT. The Coulomb potential of the electron localized at the cluster keeps the other electrons from flowing through the tunnel junction. Tunnel current increase is possible only after a discrete increase of bias voltage, what is observed as a so called Coulomb staircase in I-V curves. In our investigations, we have created an ultra-thin oxide (barrier) layer on the Si(111) 7x7 surface via controlled oxidation process inside the UHV chamber. One of the tunnel junctions was made by deposition of Ag nanoclusters onto an oxidized Si(111) surface. The other tunnel junction was set up by STM tip and vacuum when the tip was hovering over the Ag cluster. I-V curves measured in above clusters showed a step-like shape. The steps were smeared due to thermal broadening and asymmetry in capacitances and resistances of both tunnel junctions. The junction parameters were estimated by fitting the experimental curve to the theoretical one.

Keywords: Coulomb blockade, Coulomb staircase, clusters, double tunnel junction, STM

1. INTRODUCTION

The number of transistors in integrated systems (IC) is increasing twice every 18 months according to Moore's law. This tendency is kept for more than 40 years of IC production history [1]. However, achieving a higher integration scale becomes difficult due to some physical limits e.g. quantum effects leading to more effective dissipation of charge carriers in the conductive channel of the Field Effect Transistor (FET). Therefore, further progress in miniaturization of IC needs new ideas and technologies. One of the new ideas is using the Coulomb Blockade (CB) effect which should enable us to control the flow of individual electrons within the systems which include small metallic clusters between source and drain electrodes. The first experiments with the Coulomb Blockade (CB) effect were performed already in the sixties of the XX-th century [2] in tunnel junctions of ultra small capacitances. The first theory, so called orthodox theory was elaborated in 1975 [3]. The development of nanotechnology in the eighties enabled the creation of the double tunnel junctions with the precise location of the small clusters between two outer electrodes. It was the beginning of so-called "single electronics" or single electron tunneling (SET) devices [4, 5, 6]. The quick development of nanotechnology creates a demand for a new type of more accurate measuring apparatus and new standards. The progress in SET electronics observed during the last decade [7, 8] gives us hope that the Coulomb Blockade effect may be used for the creation of current intensity standards in the near future [9]. Scanning Probe Microscopy (SPM) created another wide branch of modern analytical techniques enabling versatile characterization of surfaces and nanostructures, including their local density of electronic states resolved at the nanoscale [10]. In our investigations, we have created an ultra-thin oxide (barrier) layer on the Si(111)

7x7 surface via a controlled oxidation process inside the UHV chamber. Creation of the first tunnel junction was achieved via deposition of Ag nano-clusters onto an oxidized Si(111) surface. The second tunnel junction was created using a STM tip and vacuum barrier. I-V curves measured above the Ag clusters showed step-like curve. The steps were smeared due to thermal broadening and asymmetry in capacitances and resistances of both tunnel junctions. Double-junction parameters were estimated fitting the experimental curve to the theoretical one.

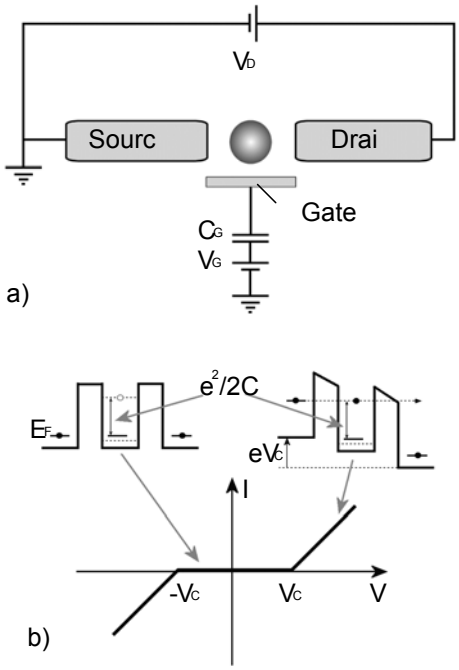

Fig. 1. (a) The scheme of single electron transistor with small cluster placed between the source and drain electrodes; (b) I-V characteristic exhibiting the Coulomb blockade effect and the energy diagram for non biased (left) and biased (with V_C potential) double tunnel junction.

2. COULOMB BLOCKADE EFFECT

As mentioned in the Introduction, the first experiments showing the CB effect were performed in late sixties of the XX-th century using planar tunnel junctions with ultra-small metallic grains embedded in the thin oxide layer [2, 11]. The first quantitative theory on the correlated tunneling of the individual electrons was elaborated by Kulik et al. [3] in 1975. The experimental methods at these times did not allow creation of the individual nanodots and placing them at strictly desired spots located between two outer electrodes. The new techniques developed in the eighties as molecular beam epitaxy (MBE), different methods enabling nanoclusters' creation and SPM methods for nanostructures' imaging and characterization lead to quick development of so called "single electronics". The double tunnel junction with a small metallic island (cluster) placed between two other electrodes is the simplest single-electron device. The scheme of such a device is shown in Fig. 1a.

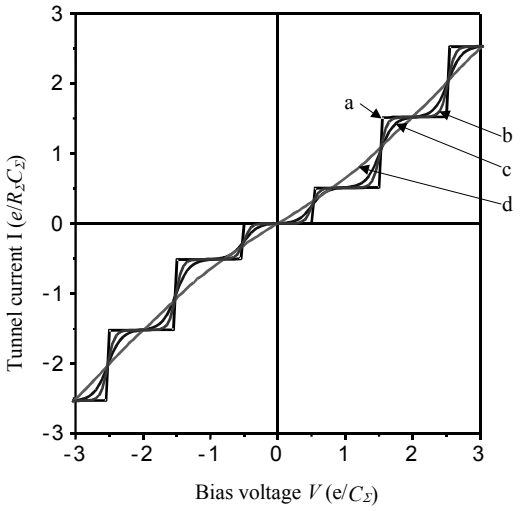

Fig. 2. Coulomb blockade and Coulomb staircase effects in the double tunnel junction with a central small metallic island for different values of k_BT/E_C ratio. The junction parameters are as follows: $C_2/C_1 = 100$, $R_2/R_1 =$, $Q_0 = 0$, $C = C_1 + C_2$, $R = R_1 + R_2$. The individual curves (a-d) were calculated using the SETTRANS software available at web page: http://hana.physics.sunysb.edu/set/software/ for $k_BT/E_C = 0$; 0.05; 0.1 and 0.5 respectively.

Electrically isolated nano-clusters between two outer electrodes exhibit capacitances of atto- or even sub-attofarads. The charging energy $E_C = e^2/2C$ for an individual electron to be placed at the cluster may be higher than the electron's thermal energy k_BT. The Coulomb potential created after charging the cluster blocks the other electrons flow through the tunnel junction. Tunnel current increase is possible after a discrete increase of bias voltage (≡ delivering the activation energy E_a to the system) only, and I-V curves at the 0 K limit exhibit sharp steps called Coulomb staircase as shown in Fig. 2, curve a. The finite temperature causes the smearing of the sharp steps and the curves b, c and d in the Fig. 2 exhibit the cases for (k_BT/E_C)= 0.05, 0.01 and 0.5 respectively. The steps disappeared at the latter case. The capacitances and resistances between electrodes and cluster on both sides (C_1, C_2 and R_1, R_2 respectively) usually are not equal. Their ratios (C_1/C_2 and R_1/R_2) influence the slopes of the lateral and vertical parts of the I-V curves' steps as seen in Fig.3a and 3b.

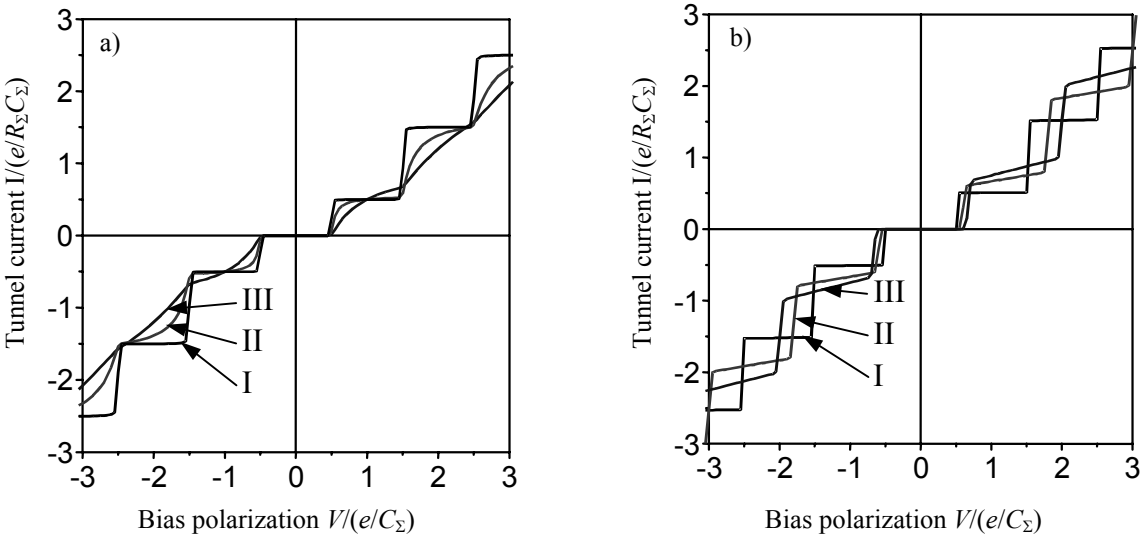

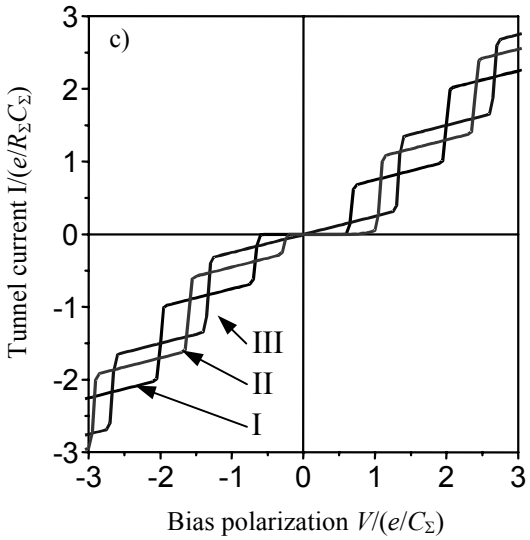

Fig. 3. Coulomb blockade and Coulomb staircase effects in the double tunnel junction with the central small metallic island for different values of parameters:
a) I-V curves calculated for different values of R_2/R_1 ratio (1 - I, 10 - II, 10^3 - III);
Remaining parameters are: $C_2/C_1 = 10^3$, $Q_0 = 0$, $k_BT/E_C = 10^{-2}$.
b) I-V curves calculated for different values of C_2/C_1 (3 - I, 10 - II, 10^2 - III);
Remaining parameters are: $R_2/R_1 = 10^6$, $Q_0 = 0$, $k_BT/E_C = 10^{-2}$.
c) I-V curves calculated for different values of Q_0 (0e - I, 0.3e - II, 0.5e - III);
Remaining parameters are: $R_2/R_1 = 10^6$ $C_2/C_1 = 10^2$, $k_BT/E_C = 10^2$.

Equalizing the Fermi level between two metals coming to the contact appears due to charge transfer from the metal characterized with smaller work function to the one with higher work function. In the case of the double tunnel junction, equalizing the Fermi levels is possible for discrete values of energy. For such a system, we can estimate the charge localized on the island, so called "polarization charge", using the dependence $Q_0 = CV_G$. This polarization charge does not have to be associated with a discrete number of electrons as it is due to rearrangement of the electron gas with the respect to the positive background of ions and as such it may take on a continuous range of values. The discrete nature of an electron charge becomes apparent when we consider changes in this due to the tunneling of a single electron. Usually there exists a polarization charge in the system which is a fractional part of the elementary charge and usually is smaller than e/2. The polarization charge localized on the island leads to narrowing of the CB effect what is illustrated in Fig. 3c. Quantum size effects (QSE) may appear when the island dimensions become comparable to the electron's de Broglie wavelength. The appropriate energy component is $E_k = 1/g(E_F)V_w$, where $g(E)$ represents the density of electron states at the Fermi level and V_W is the island volume. QSE and CBE may have comparable contribution to the activation energy of the system which may be expressed by the sum:

$$E_a = E_C + E_k \tag{1}$$

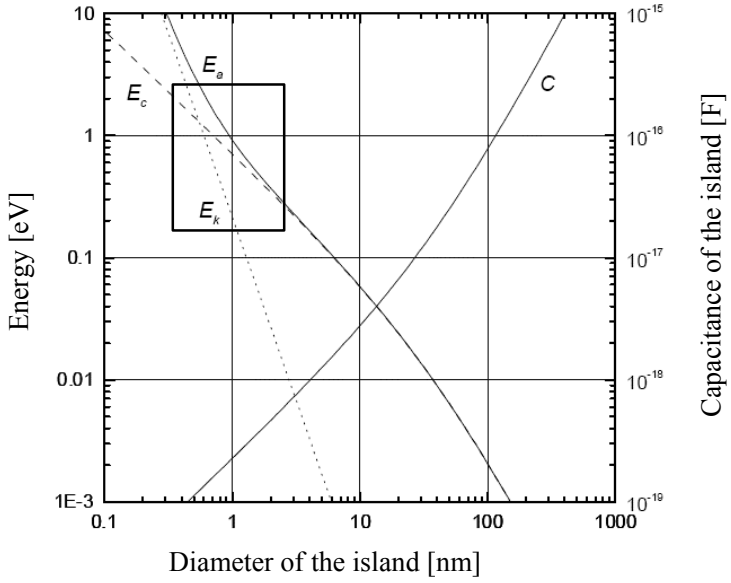

Fig. 4. Activation energy E_a (——) and its components: Coulomb charging energy E_C (- - - -) and kinetic energy of the electron based on QSE E_k (· · · · ·) calculated in the case of a simple model, where the island is recognized as an ideal sphere placed on non-conducting substrate with the dielectric constant $\varepsilon = 4$. It is assumed that the channel where tunneling takes place is of 10% of the island surface and the potential barrier thickness is about 2 nm. The spot surrounded by thick black line corresponds to those energy and island dimension parameters for which the STM may be used to search for CB and QS effects.

Figure 4 shows graphically both components of E_a as a function of the Coulomb island diameter and one can see that E_k is comparable to E_C for small islands of sub-nanometer diameter. The QSE may disturb the uniformity of the CB staircase and should be taken into consideration in such a case. The curve C represents the island's capacitance vs. one of the electrodes as a function of island diameter (the right axis represents the capacitance values).

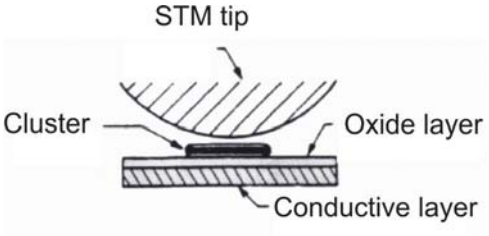

Fig. 5. Diagram of the double tunnel junction with the STM tip as one of the conductive electrode.

3. EXPERIMENTAL DETAILS

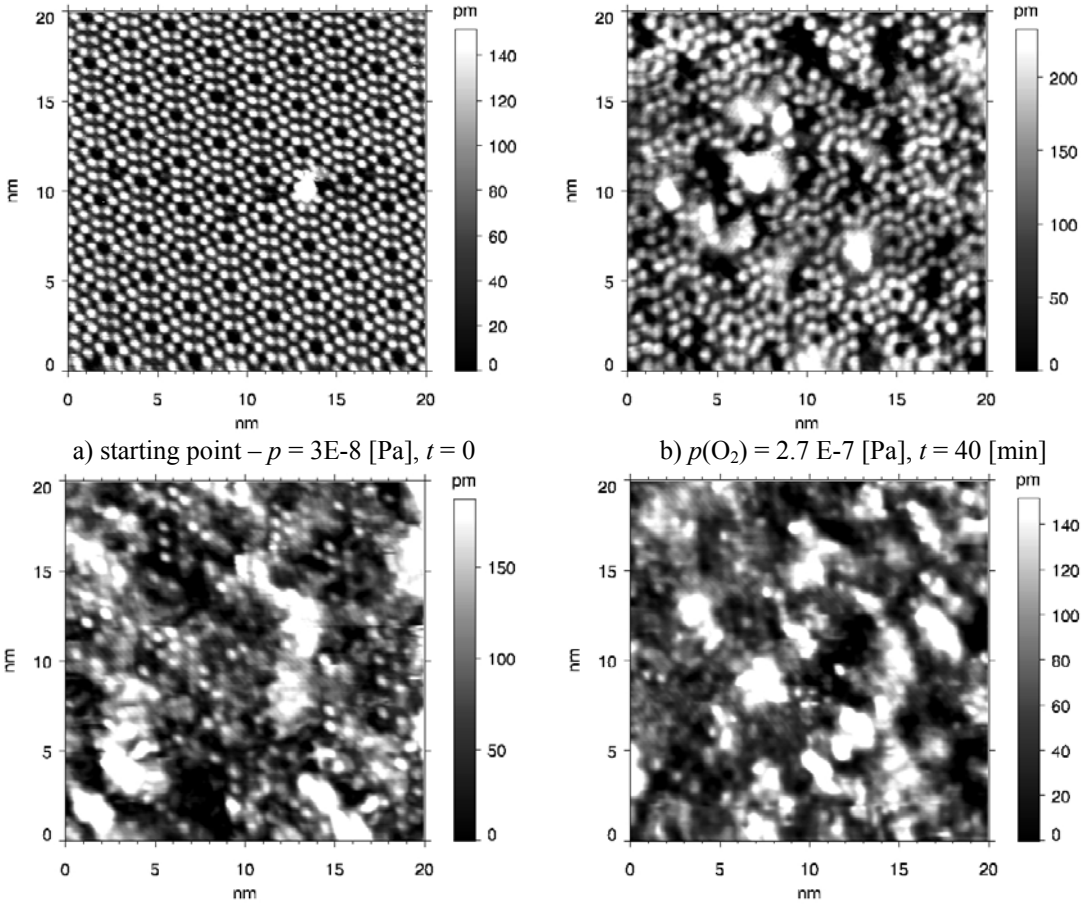

Fig. 6. STM images (20 nm × 20 nm) recorded during the oxidation process of the Si(111) 7x7 substrate. The oxygen partial pressure and time of exposure are indicated above every STM image. The total time of exposure was 122 min[12].

In this study, the double tunnel junction was created with the help of an STM tip, vacuum barrier and a metallic cluster deposited onto n-doped Si(111) substrate covered with an ultra thin silicon oxide layer. The Si(111) sample was flashed at ultra high vacuum (UHV) conditions to create a clean and reconstructed (7x7) surface. The substrate was oxidized by exposure of the substrate to a pure (99,9999%) oxygen gas in UHV chamber. Oxygen pressure and purity were controlled by means of a residual gas analyzer (RGA) on the 10^{-7} [Pa] level. The progress of the oxidation process was controlled by means of STM in real time. The oxidation process was stopped as soon as the 7x7 reconstruction on the Si(111) substrate was no more visible.

a) b)

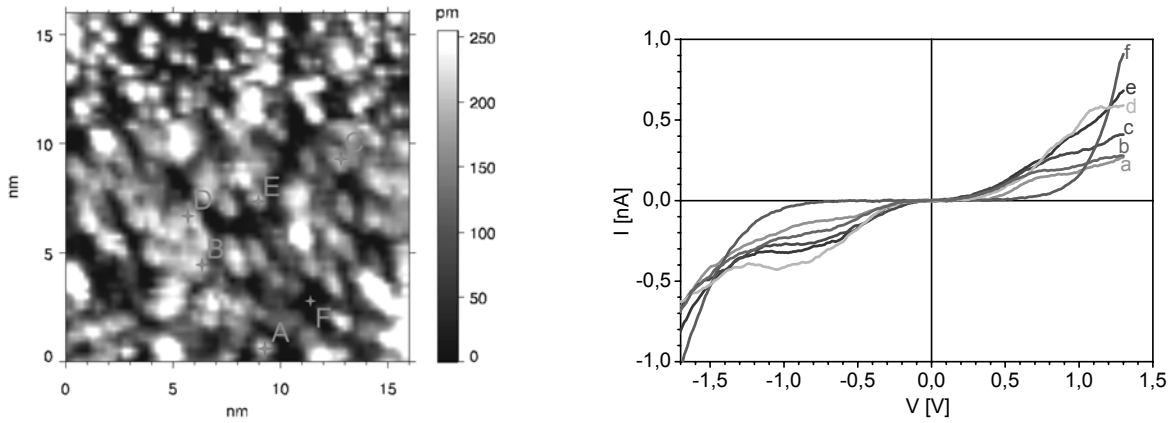

Fig. 7. a) STM topography image of the Ag clusters deposited onto SiO_x/Si(111) surface;
b) I–V curves measured above Ag clusters (a-e) and above the substrate (f).

Figure 7 shows STM images recorded consecutively during the oxidation process. The Ag clusters were grown on the oxidized silicon substrate using the EFM4 evaporation source from OMICRON-Nanotechnology GmbH. The source enables the precise control of the evaporated material flux on sub-monomolecular coverage level. The substrate temperature was kept at about 475 K and the pressure in the UHV chamber during Ag evaporation was kept at 1.33×10^{-7} [Pa]. The I-V curves were measured at individual spots of the sample or at every topography point using the current imaging tunneling spectroscopy (CITS) method. During CITS measurements the scanning probe (STM tip) is stopped, the electronic feedback loop which controls the tunnel current intensity (and the probe-sample distance during scanning) is off and the I-V characteristic is measured in the desired range of the bias voltage.

4. RESULTS AND DISCUSSION

Figure 7a shows the STM topography image of an oxidized silicon substrate after deposition of small amount of Ag. It is difficult to differentiate small Ag clusters of 1 to 2 nm in diameter on the corrugated substrate. Nevertheless, the roughness analysis leads us to the conclusion that most of observed protrusions represent small Ag clusters. The roughness is defined as:

$$R_{RMS} = \sqrt{\frac{1}{N}\sum_{1}^{N}\left(z - z_{avg}\right)^2}\ , \tag{2}$$

where N is number of data points with given z and z_{avg} is the mean z value.

Table 1. The double junctions' parameters fitted to I-V curves (a-e) shown in Fig. 7c using the SETTRANS software [12].

	C_1 [10^{-19} F]	C_2 [10^{-19} F]	R_1 [10^9 Ω]	R_2 [10^9 Ω]	Q_0
a	1,63	0,33	0,84	4,19	0,08e
b	1,72	0,16	0,22	1,94	0
c	1,49	0,08	0,06	3,05	0,05e
d	1,14	0,1	0,52	2,63	0,03e
e	1,58	0,14	0,29	2,61	0

The root mean square (RMS) roughness for the oxidized substrate, as seen in Fig. 6d, was equal to 0.035 [nm]. The roughness increased up to 0.085 [nm] after Ag deposition (more than 100%). The detailed analysis of I-V curves measured above Ag clusters revealed the

step-like shape contrary to I-V curves measured at other spots. The I-V curves measured at spots marked by crosses in the topography image are shown in Fig. 7b. Some of the stepped I-V curves shown in Fig. 7b were analyzed using SETTRANS software to estimate the double tunnel junction's parameters as capacitances (C_1, $C_{2)}$, resistances (R_1, R_2) and the residual charge on the island. The estimated parameters are presented in Table 1.

Parameters values are of expected order e.g. of attofarads and gigaohms. The individual experimental I-V curves measured above the Ag clusters and the numerically fitted curves are presented in Fig. 8 showing high conformity between them. The steps are not as sharp as the ideal curve at the 0 K limit shown in Fig. 3 but we have to remember that the I-V measurements were performed at room temperature with $k_BT/E_C \approx 0.1$. Curves a and c in Fig. 8 are not symmetric vs. 0 V of bias voltage. This asymmetry is caused by the presence of a polarization charge on the metallic island (0.08e and 0.05e respectively). The thickness of the oxide layer was estimated using the simple formula $C = \varepsilon_0\varepsilon_r S/d$, where ε_0 - permittivity of the free space, ε_r - relative permittivity, S - tunneling channel estimated as 10% of the island area, and d - the insulator thickness. Assuming that: capacitance for the cluster-substrate junction with the cluster diameter of 1.3 [nm] is $C_2 = 0.08\times10^{-19}$ [F], SiO_x relative permittivity $\varepsilon_r = 4$, tunneling channel $S = 0.13$ [nm^2], the oxide layer thickness was estimated to be of about 0.6 [nm], that means about 2 ML. This result would confirm that the goal to create an ultra thin oxide layer enabling the observation of a CBE and CB staircase on I-V curves at room temperature in the double tunneling junctions was achieved.

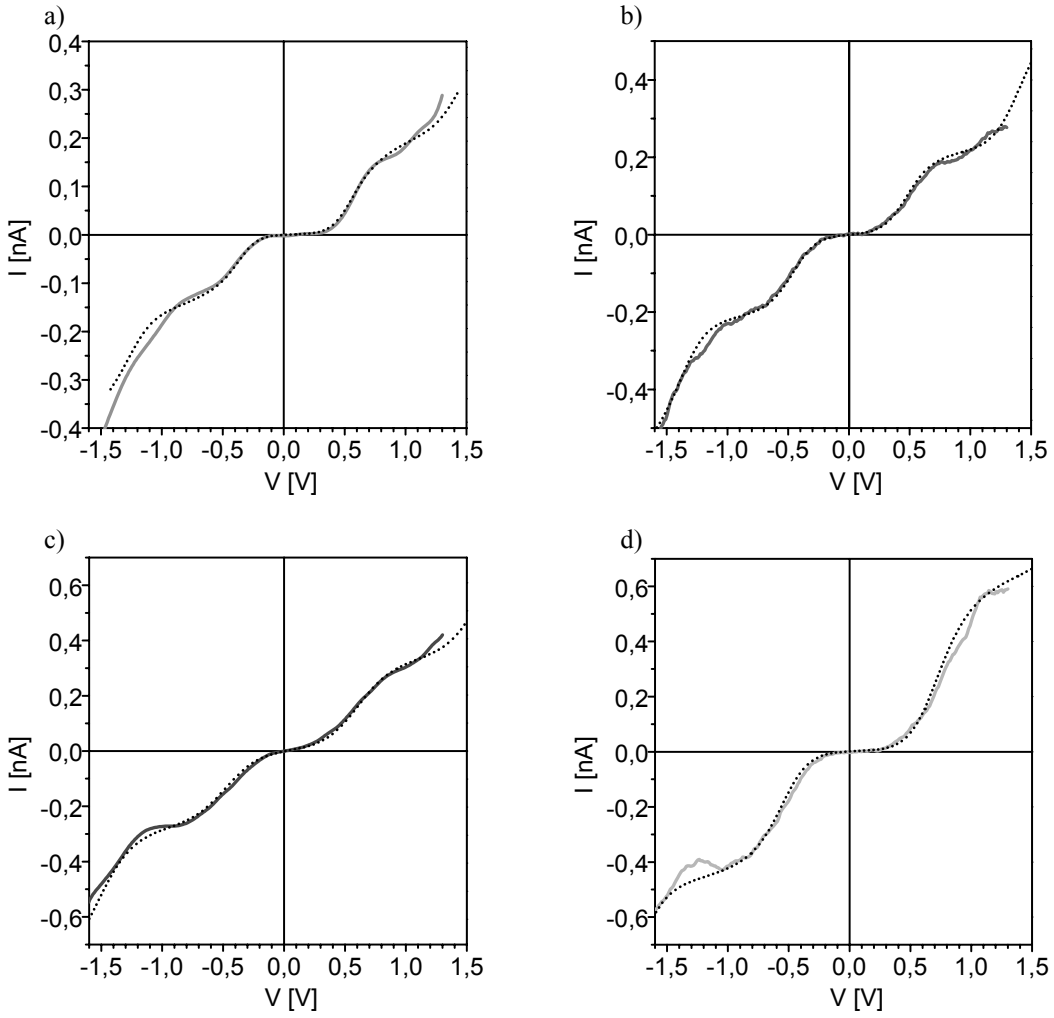

Fig. 8. The set of I-V curves measured above Ag clusters shown in Fig. 7 (curves a - d) – continuous line and fitted curves - dotted line, using parameters R_1, R_2, C_1, C_2 and Q_0 shown in Table 1 [12].

5. CONCLUDING REMARKS

Double tunneling junctions were created via controlled oxidation of n-Si(111) substrate, subsequent Ag cluster deposition, and with an STM tip as a second conductive electrode separated by a vacuum barrier from the Ag cluster. CBE and CB staircases were observed on I-V curves at room temperature if the central electrode (Ag cluster) diameter was of 1 nm order and the oxide layer thickness was of a few ML. The relevant parameters characterizing the double tunnel junction were estimated via fitting the experimental curves to the theoretical model. The Coulomb blockade effect may play a crucial role in further development and miniaturization of future electronic devices.

ACKNOWLEDGEMENTS:

This work was supported by the Ministry of Scientific Research and Information Technology (Project No. 2P03B 042 25).

REFERENCES

1. Moore G.E., Electronics 38(8), 1965.
2. Lambe J., Jaklevic R. C., Phys. Rev. Lett. 20, p. 1504, 1969.
3. Kulik O., Shekhter R. I., Sov. Phys. JETP 41, p. 308, 1975.
4. Hanna E., Tinkham M., Phys Rev. B 44, p. 5919, 1991.
5. Single Charge Tunneling, vol. 294 of NATO Advanced Study Institute, Series B: Physics, edited by H. Grabert, M.H. Devoret (Plenum, New York, 1992).
6. Schon G., Quantum Transport and Dissipation, edited by T. Dittrich et al, chapter 3 (Wiley-VCH Verlag, 1998).
7. Rainer Waser, Nanoelectronics And Information Technology: Advanced Electronic Materials and Novel Devices, John Wiley & Sons Inc; 02/2005.
8. Takahashi Y., Ono Y., Fujiwara A., Inokawa H., J. Phys.: Condens. Matter 14, R995, 2002.
9. Likharev K. K., Zorin A. B., J. of Low Temp. Phys. 59, pp. 347-382, 1985.
10. Meyer E., Hug H. J., Bennewitz R.: *Scanning Probe Microscopy – The Lab on a Tip*, Springer-Verlag, Berlin, 2003.
11. Giaver, Zeller H. R., Phys. Rev. 181, p. 789, 1969.
12. Gutek J.: Ph.D Thesis, *Creation of metallic nanostructures at Si(111) substrate and theirs characterization by means of scanning tunneling microscopy and spectroscopy*, Poznań 2005.

BADANIA ZJAWSKA BLOKADY KULOMBOWSKIEJ W PODWÓJNYCH ZŁĄCZACH TUNELOWYCH

Streszczenie

Pierwsze eksperymenty, w których obserwowano efekty blokady kulombowskiej związanej z tunelowaniem elektronów w strukturach o ultra – małych pojemnościach elektrycznych, przeprowadzano już w latach sześćdziesiątych XX wieku. W 1975 roku opracowana została pierwsza tzw. „ortodoksyjna" teoria, która ilościowo opisywała zjawisko przepływu prądu w podwójnych złączach tunelowych. Szybki rozwój nanotechnologii w latach osiemdziesiątych ub. wieku umożliwiły wytwarzanie podwójnych złączy tunelowych poprzez precyzyjne umieszczanie małych metalicznych klasterów pomiędzy dwiema zewnętrznymi elektrodami. Był to początek szybkiego rozwoju dziedziny nazywanej obecnie „elektroniką jednoelektronową" – czyli taką która wykorzystuje własności wynikające z przepływu pojedynczych elektronów. Elektrycznie izolowane nano-klastery umieszczone między zewnętrznymi elektrodami wykazują pojemności rzędu attofaradów. Energia ładowania równoważnego kondensatora $(E_C = e^2/2C)$ czyli energia, którą potrzebuje elektron, aby zostać ulokowanym w nanoklasterze jest wtedy większa od energii termicznej k_BT. Potencjał kulombowski powstały po naładowaniu klastera blokuje przepływ kolejnych elektronów przez złącze tunelowe. Wzrost prądu tunelowego

jest możliwy tylko po zwiększeniu napięcia polaryzacji o pewną skwantowaną wielkość, co prowadzi do pojawienia się tzw. stopni kulombowskich na charakterystyce I-V.

W naszych badaniach, wytworzyliśmy ultra-cienką warstwę tlenku krzemu (bariera potencjału) na powierzchni krzemu Si(111) 7x7 w procesie kontrolowanego utleniania w komorze bardzo wysokiej próżni. Pierwsze złącze tunelowe utworzono poprzez osadzenie nanoklasterów srebra na utlenionej powierzchni krzemowego podłoża. Drugie złącze, z barierą próżniową, tworzone było poprzez lokalizację sondy mikroskopu tunelowego nad klasterem Ag. Zmierzone nad klasterami Ag charakterystyki I-V wykazały obecność stopni kulombowskich. Rozmycie stopni i ich nachylenie wynikało z poszerzenia termicznego oraz asymetrii pojemności i rezystywności obu złączy tunelowych. Oszacowano parametry podwójnych złączy tunelowych poprzez dopasowanie krzywych eksperymentalnych do zależności teoretycznych.

Efekt blokady kulombowskiej może być wykorzystany w elektronice ze względu na ekstremalną czułość ładunkową w różnego rodzaju miernikach oraz w układach pamięci o ekstremalnie dużych gęstościach upakowania elementów.